

Probing time orientability of spacetime

N.A. Lemos,^{1,*} D. Müller,^{2,†} and M.J. Rebouças^{3,‡}

¹*Instituto de Física, Universidade Federal Fluminense, Av. Litorânea, S/N
24210-340 Niterói – RJ, Brazil*

²*Instituto de Física, Universidade de Brasília 70919-970 Brasília - DF, Brazil*

³*Centro Brasileiro de Pesquisas Físicas, Rua Dr. Xavier Sigaud 150
22290-180 Rio de Janeiro – RJ, Brazil*

(Dated: November 3, 2022)

Abstract

In general relativity, cosmology and quantum field theory, spacetime is assumed to be an orientable manifold endowed with a Lorentz metric that makes it spatially and temporally orientable. The question as to whether the laws of physics require these orientability assumptions is ultimately of observational or experimental nature, or the answer might come from a fundamental theory of physics. The possibility that spacetime is time non-orientable lacks investigation, and so should not be dismissed straightaway. In this paper, we argue that it is possible to locally access a putative time non-orientability of Minkowski empty spacetime by physical effects involving quantum vacuum electromagnetic fluctuations. We set ourselves to study the influence of time non-orientability on the stochastic motions of a charged particle subject to these electromagnetic fluctuations in Minkowski spacetime equipped with a time non-orientable topology and with its time orientable counterpart. To this end, we introduce and derive analytic expressions for a statistical time orientability indicator. Then we show that it is possible to pinpoint the time non-orientable topology through an inversion pattern displayed by the corresponding orientability indicator, which is absent when the underlying manifold is time orientable.

PACS numbers: 03.70.+k, 05.40.Jc, 42.50.Lc, 04.20.Gz, 98.80.Jk, 98.80.Cq

* nivaldolemos@id.uff.br

† dmuller@unb.br

‡ reboucas.marcelo@gmail.com

I. INTRODUCTION

In relativistic cosmology and quantum field theory spacetime is described as a four-dimensional differentiable manifold, a topological space with an additional differentiable structure that permits to locally define connections, metric and curvature with which the gravitation theories and the dynamics of other fields are locally formulated. So, two important elements in the mathematical description of the Universe and in the local dynamics of the (micro) physical laws are the geometry and the topology of the underlying spacetime manifold.

Topologically inequivalent manifolds can have the same geometry; conversely, a fixed topological space can have different geometries. So, for example, Kasner, Gödel, plane-wave and Minkowski geometries all can have \mathbb{R}^4 as underlying manifold, whereas the manifold $\mathbb{S}^2 \times \mathbb{R}^2$, admits, for example, Reissner-Nordström and Schwarzschild solutions of Einstein's field equations, which represent physically different gravitational fields [1, 2].

Geometry is a local attribute that brings about curvature. Topology is a global property of manifolds that requires consideration of the entire manifold. So, for example, compactness is a global property: it cannot be mathematically formulated in local terms. Simple-connectedness and orientability are examples of other topological properties of spacetime manifolds. They do not arise from local mathematical knowledge alone. This is a mathematical issue. However, if local physics is brought into the scene, it can play a key role in the local access to the topological properties of spacetime. This is the main concern of this work, which focuses on the time orientability of spacetime.

The most primary definition of orientability arises in the context of a topological space. However, when extra structure is added to the topological manifold, different formulations of orientability can be given. Thus, for example, the Möbius band \mathbb{M}^2 and the Klein bottle \mathbb{K}^2 are non-orientable as topological spaces. When endowed with Lorentz metrics, two possible types of orientability (non-orientability) come about: spatial or temporal orientability (non-orientability), depending on the way the manifolds are equipped with a Lorentz metric. These examples make it apparent that whether a spacetime is time or space orientable may be looked upon as a joint topological-geometrical property, in the sense that it depends on the topology of the underlying manifold but also on the specific Lorentz metric we equip the manifold with [2, 3].

Most illustrations of non-orientability we encounter depict *spatial* non-orientability by making use of spatial paths which bring a traveler back to her/his starting point with left- and right-hand sides exchanged (mirror-reversed) [4]. So, for example, in the Wikipedia entry “Orientability” [5] the crab’s left and right claws are reversed when it makes a round (*spatial*) trip along the Möbius band. However, the illustration of *time* non-orientability would be trickier, as it deals with an inversion (flip) of the time t after a round-trip over the whole manifold. We are familiar with left and right exchanges, but not with clocks first running forward then backward in time after a circumnavigation. Yet, the Möbius band \mathbb{M}^2 can also be used as an example of *time* non-orientability as long as one suitably endows it with time and space coordinates t, x such that time is inverted (flips) after a circumnavigation (translation along the x -direction). This is a periodic time inversion of topological origin.

It is generally assumed that the spacetime manifolds one deals with in physics are orientable as topological manifolds and are additionally endowed with an appropriate Lorentz metric, making them separately time and space orientable.¹ Non-orientability raises intriguing questions, and it is generally seen as an undesirable feature in physics. Yet, space and time non-orientability of Lorentzian spacetime manifolds are concrete mathematical possibilities for the physical spacetime. On the other hand, severe orientability assumptions could risk ruling out something that the spacetime topology might be trying to “tell” us, and it might also discourage further investigations on the interplay of physics and topology. Thus, it seems reasonable to expect that the ultimate answer to questions regarding the orientability of spacetime should rely on local experiments or cosmological observations, or even might come from a fundamental theory of physics.

In this article we address the question as to whether one can empirically and locally access the putative topological property of *time* non-orientability (orientability) of spacetime manifolds \mathcal{M}_4 .²

Since the net role played by time orientability is more clearly ascertained in static flat spacetime, whose dynamical degrees of freedom are frozen, in this work we focus on

¹ Theoretical arguments in support of these orientability assumptions combine space and time universality of local physical laws with the thermodynamically defined local arrow of time, charge conjugation and parity (CP) violation and CPT invariance [1, 2, 6]. The impossibility of having globally defined spinor fields on non-orientable spacetime manifolds is also often used in favor of these orientability assumptions [1, 2, 7–10]. It should be noted, however, that time universality can be looked upon as a topological assumption of global time homogeneity. This topological assumption rules out time non-orientability from the outset.

² The nature of time and the existence of various arrows of time are contested issues, which we evade in this paper, in which we assume that time is real and passes in all scales. The literature on this debate is fascinating and vast, but for the sake of brevity we refer the readers to Refs. [11, 12] and references therein, including the books [13–16].

Minkowski spacetime. The physical system that turns out to be suitable to play the revealing role of global time non-orientability is a non-relativistic charged particle locally subjected to quantum vacuum fluctuations of the electromagnetic field.³

To show that one can access time orientability, we investigate signatures of time non-orientability through the stochastic motions of a charged test particle under electromagnetic quantum fluctuations in Minkowski spacetime \mathcal{M}_4 with time non-orientable topology and in its time orientable counterpart. The time orientability statistical indicator that we introduce combines geometrical-topological properties with the dynamics of the above specific physical system engineered to test orientability.

The structure of the paper is as follows. In Section II we set up the notation and present some key concepts and results regarding topology of manifolds, which will be needed in the remainder of the paper. In Section III we present the physical system along with the background geometry and topology. In Section IV we introduce the time orientability statistical indicator and derive its expressions for a charged particle under quantum vacuum electromagnetic fluctuations in Minkowski spacetime equipped with temporally non-orientable and orientable topologies. We show that a comparison of the time evolution of our statistical indicators for these cases allows one to discriminate the orientable from the non-orientable topology. Time non-orientability can be locally unveiled by the inversion pattern of the curves of the time orientability statistical indicator for a point charge under quantum vacuum electromagnetic fluctuations. In Section V we present our main conclusions and final remarks.

II. CONTEXT AND MATHEMATICAL PRELIMINARIES

To make this work to a certain extent self-contained, in this section we define the notation, give some basic definitions and present a few results concerning the topology of the manifolds which are used throughout this paper.

We first briefly underscore the context of this article vis-à-vis some recent works involving spacetimes with a nontrivial topology. For both the spatially flat Friedmann-Robertson-Walker (FRW) and the Minkowski spacetimes, the underlying manifold \mathcal{M}_4 is globally de-

³ In an influential work, this system was used by Yu and Ford [17] in Minkowski spacetime with a conducting plane (nontrivial spatial topology). They endeavored to shed light on the question as to whether a test charged particle would perform stochastic motions induced by quantum fluctuations of the electromagnetic field [18, 19]. Related investigations have since been made in a number of papers, including Refs. [20–28].

composable as $\mathcal{M}_4 = \mathbb{R} \times M^3$, where M^3 is the simply-connected 3-manifold \mathbb{R}^3 . However, since topologically inequivalent manifolds can have a given spacetime geometry, the underlying topology of FRW or Minkowski manifolds can belong to a set of diverse possibilities. For example, the spatial section M^3 of both spacetimes can be any quotient manifold of the form $M^3 = \mathbb{E}^3/\Gamma$, where \mathbb{E}^3 is the covering space,⁴ and Γ is a discrete group of freely acting isometries of \mathbb{E}^3 , also referred to as the holonomy [29, 30].⁵ The familiar form $\mathcal{M}_4 = \mathbb{R} \times M^3$ is very often assumed in cosmology and quantum field theory, and in particular it is adopted in cosmic topology, which investigates the spatial topology of the Universe.⁶

In the present work, rather than addressing a possible nontrivial spatial topology of the FRW spacetime, which is the subject matter of cosmic topology, we focus on a single topological property of the Minkowski spacetime manifold \mathcal{M}_4 , namely *time orientability*. Let us first point out that any simply connected spacetime manifold is both time and space orientable. Thus, perhaps the simplest way to equip Minkowski spacetime with time non-orientability is by taking

$$\mathcal{M}_4 = \mathcal{M}^2 \times \mathbb{E}^2, \quad (1)$$

where \mathcal{M}^2 is a two-dimensional time non-orientable quotient manifold, $\mathcal{M}^2 = \mathbb{E}^{2,1}/\Gamma$, where $\mathbb{E}^{2,1}$ denotes the simply-connected plane equipped with a Lorentz metric, that is, Minkowski two-dimensional spacetime. It follows that the orientability of \mathcal{M}_4 reduces to the orientability of \mathcal{M}^2 .⁷

To make a suitable choice of \mathcal{M}^2 , we start by reviewing some basic results concerning Euclidean two-dimensional manifolds and then proceed to choose a non-orientable Lorentzian two-dimensional manifold. A first question we address is the identification of all topologically inequivalent Euclidean two-dimensional manifolds.

The simplest example of a two-dimensional Euclidean manifold with nontrivial topology is the cylinder \mathbb{C}^2 , whose construction as a quotient manifold, $\mathbb{C}^2 = \mathbb{E}^2/\Gamma$, is such that a point $P = (x, y)$ of the cylinder is obtained from the covering manifold \mathbb{E}^2 by identifying the points that are equivalent under the action of the elements γ_i of the covering isometry group Γ . Specifically, a point $P = (x, y)$ of the cylinder is the equivalence class of all points P' in the covering space \mathbb{E}^2 such that $P' = \{(x + n_x a, y) \mid n_x \in \mathbb{Z}, a = \text{const}\}$, or $P \equiv P' = \gamma_i P$ with

⁴ \mathbb{E}^n is \mathbb{R}^n endowed with the Euclidean metric.

⁵ Refs. [31–34] give a detailed account of the classification of flat 3-dimensional Euclidean topologies.

⁶ For review papers on cosmic topology and recent observational constraints, see Refs. [35–49].

⁷ A mathematically much more involved way would be by the decomposition $\mathcal{M}_4 = \mathbb{K}^3 \times \mathbb{R}$ with the time t chosen as the flipped direction of the 3-dimensional non-orientable Klein space [4, 29–34].

$\gamma_i \in \Gamma$ being a translation by a in the direction of the x -axis. A convenient way to visualize a quotient manifold is through the so-called fundamental domain (cell) or fundamental polygon. For the cylinder \mathbb{C}^2 the fundamental cell is a strip of \mathbb{E}^2 bounded by parallel lines, say $x = 0$ and $x = a$, that are identified through translations to form the cylinder \mathbb{C}^2 . The cylinder \mathbb{C}^2 is a surface (two-manifold) lying in three-dimensional space. This embedded view, however, does not necessarily work for other Euclidean two-manifolds.

A very important advantage of the quotient construction, \mathbb{E}^2/Γ , comes from examples of 2-manifolds that cannot be properly displayed in the regular three-dimensional space. The twisted cylinder \mathbb{C}^{*2} is one example of this kind of manifold. It cannot lie in ordinary three-dimensional space without intersecting itself. Yet it has a rather simple representation as a quotient manifold. Indeed, it is obtained from a strip of \mathbb{E}^2 bounded by parallel lines which are identified through a glide reflection: translation followed by a flip (inversion).⁸ A point $P = (x, y)$ of the twisted cylinder \mathbb{C}^{*2} represents a set of points in the covering space \mathbb{E}^2 of the form $P' = \{(x + n_x a, (-1)^{n_x} y) \mid n_x \in \mathbb{Z}, a = \text{const}\}$ or $P \equiv P' = \gamma_i P$ with $\gamma_i \in \Gamma$ being translation by a in the x -direction followed by an inversion (flip) in the y -direction, a single glide reflection.

Finally the last two-dimensional quotient Euclidean manifolds are the torus \mathbb{T}^2 and the Klein bottle \mathbb{K}^2 . Both can be obtained through identification of opposite sides of a rectangle. The torus and the Klein bottle are related quite in the same way as the cylinder and the twisted cylinder. For this reason, the Klein bottle is also known as the twisted torus [50]. A point $P = (x, y)$ of the torus \mathbb{T}^2 represents the equivalence class of all points in the covering manifold \mathbb{E}^2 such that $P' = \{(x + n_x a, y + n_y b) \mid n_x, n_y \in \mathbb{Z}, a, b = \text{const}\}$, or $P \equiv P' = \gamma_i P$ with $\gamma_i \in \Gamma$ being a translation by a in the x -direction and by b in the y -direction. As for the Klein bottle, one has $P \equiv P' = \{(x + n_x a, (-1)^{n_x} y + n_y b) \mid n_x, n_y \in \mathbb{Z}, a, b = \text{const}\}$.

It can be shown that, under the assumptions of completeness and connectedness, there are no other Euclidean two-dimensional manifolds of the form \mathbb{E}^2/Γ (quotient manifolds) than the above-mentioned four [51]. Actually, any other group Γ yields a quotient space that is not a manifold [51]. Moreover, \mathbb{E}^2 and these four Euclidean quotient manifolds are connected and complete (Euclidean metric). It turns out that connectedness and completeness exclude

⁸ A popular, but not entirely accurate, embedded representation of the twisted cylinder is by means of the well known Möbius band \mathbb{M}^2 , which is obtained through the identification of two opposite sides of a rectangle after a flip (half twist). The Möbius band is visually useful as it can lie in three-dimensional space, but it is *not* a regular manifold since it has a boundary. The twisted cylinder \mathbb{C}^{*2} , on the other hand, is a quotient manifold $\mathbb{C}^{*2} = \mathbb{E}^2/\Gamma$, but cannot lie in \mathbb{R}^3 .

all Euclidean two-dimensional manifolds except for the previously mentioned quotients \mathbb{E}^2/Γ and \mathbb{E}^2 itself. This is an instance of the Killing-Hopf theorem, which ensures that, apart from \mathbb{E}^2 , each connected, complete Euclidean two-dimensional manifold is either a cylinder, twisted cylinder, torus or Klein bottle [51].

Let us move on to another important topological feature of Euclidean manifolds we use in this work. In dealing with topological manifolds we have the concept of *global homogeneity* of topological origin. A way to characterize global homogeneity of the quotient manifolds $\mathcal{M}^2 = \mathbb{E}^2/\Gamma$ is through distance functions. Indeed, for any point $\mathbf{x} \in \mathcal{M}^2$ the distance function $\ell_\gamma(\mathbf{x})$ for a given $\gamma \in \Gamma$ is defined by

$$\ell_\gamma(\mathbf{x}) = d(\mathbf{x}, \gamma\mathbf{x}) , \tag{2}$$

where d is the two-dimensional Euclidean metric. The distance function provides the length of the closed geodesic that passes through \mathbf{x} and is associated with a discrete isometry $\gamma \in \Gamma$. In *globally homogeneous* manifolds the distance function for any covering isometry γ is constant. In globally inhomogeneous manifolds, in contrast, the length of the closed geodesic associated with at least one γ is non-translational and depends on the point $\mathbf{x} \in \mathcal{M}^2$, and then is not constant. When the distance between a point \mathbf{x} and its image $\gamma\mathbf{x}$ is a constant for all points \mathbf{x} and elements $\gamma \in \Gamma$ then the isometries are translations, that is, all elements of the covering group Γ in globally homogeneous manifolds are translations. This means that in these quotient manifolds the sides of the fundamental domain are identified through independent translations. Thus, in the above set of two-dimensional quotient manifolds, besides \mathbb{E}^2 , the cylinder and the torus are topologically homogeneous, whereas the twisted cylinder and the Klein bottle are globally inhomogeneous.

Orientability is another very important global (topological) property of a manifold that measures whether one can consistently choose a clockwise orientation for loops in the manifold. A path in a \mathcal{M}^2 that brings a traveler back to the starting point mirror-reversed is called an orientation-reversing path. Manifolds that do not have an orientation-reversing path are called *orientable*, whereas manifolds that contain an orientation-reversing path are *non-orientable* [4]. The Euclidean plane, cylinder and torus are orientable, whereas the twisted cylinder and the Klein bottle are non-orientable two-dimensional manifolds. For two-dimensional quotient manifolds \mathbb{E}^2/Γ , when the covering group Γ contains at least one isometry γ that is a reflection (flip) the corresponding quotient manifold is non-orientable. There-

fore, the torus is orientable but the Klein bottle is non-orientable. Clearly non-orientable manifolds are necessarily globally inhomogeneous as the covering group Γ contains a reflection, which obviously is a non-translational covering isometry.

In Table I we collect the names, symbols, generators $\gamma \in \Gamma$ together with the topological properties of orientability and global homogeneity of the two-dimensional manifolds \mathcal{M}^2 , which are possible factors of the product manifold $\mathcal{M}_4 = \mathcal{M}^2 \times \mathbb{E}^2$, which in turn we shall take as the underlying manifold to be endowed with the Minkowski spacetime metric $\eta_{\mu\nu} = \text{diag}(+1, -1, -1, -1)$.

Manifold	Symbol	Generators $\gamma_i \in \Gamma$	Orientable	Homogeneous
Cylinder	\mathbb{C}^2	1 Translation	yes	yes
Twisted cylinder	\mathbb{C}^{*2}	1 Glide reflection	no	no
Torus	\mathbb{T}^2	2 Translations	yes	yes
Klein bottle	\mathbb{K}^2	1 Transl. 1 Glide reflect.	no	no

TABLE I. Names and symbols of two-dimensional Euclidean quotient manifolds \mathbb{E}^2/Γ together with the generators γ_i of the group Γ , and two global (topological) properties: orientability and global homogeneity.

For the product manifold given by equation (1) to be time non-orientable the factor \mathcal{M}^2 has to be a Lorentzian non-orientable manifold. The Lorentz metric, on the other hand, decisively constrains the topology of the possible underlying manifolds. Thus, not every smooth manifold can be made a Lorentzian manifold. For example, the two-sphere \mathbb{S}^2 , for which the Euler characteristic $\chi = 2$, cannot have a Lorentz metric (a consequence of the “hairy ball” theorem), whereas the torus \mathbb{T}^2 , for which $\chi = 0$, can (see, for example, Ref. [58]).

It can be shown that every compact connected smooth manifold with Euler characteristic $\chi = 0$ admits a Lorentz metric [59]. For the case of two-dimensional manifolds, this ensures that both the torus \mathbb{T}^2 and the Klein Bottle \mathbb{K}^2 , for both of which $\chi = 0$, can be equipped with a Lorentz metric. It can also be proved that every n -dimensional noncompact smooth manifold admits a Lorentz metric [59]. This guarantees, in particular, that both the cylinder \mathbb{C}^2 and the twisted cylinder \mathbb{C}^{*2} can be made Lorentzian manifolds.⁹

⁹ A smooth n -dimensional manifold M with $n \geq 2$ can be endowed with a Lorentz metric if and only if either M is noncompact or it is compact and has Euler characteristic $\chi(M) = 0$ [59, 60].

III. CHARGED PARTICLE UNDER ELECTROMAGNETIC FLUCTUATIONS

From now on, we consider a point charge under quantum vacuum electromagnetic fluctuations as the physical system used to locally probe a potential time non-orientability of spacetime.

A. The physical system

Let a nonrelativistic test particle with charge q and mass m be locally subject to vacuum fluctuations of the electric field $\mathbf{E}(\mathbf{x}, t)$ in a topologically nontrivial spacetime manifold equipped with the Minkowski metric $\eta_{\mu\nu} = \text{diag}(+1, -1, -1, -1)$.

Locally, the motion of the charged test particle is determined by the Lorentz force. In the nonrelativistic limit the equation of motion for the point charge is

$$\frac{d\mathbf{v}}{dt} = \frac{q}{m} \mathbf{E}(\mathbf{x}, t), \quad (3)$$

where \mathbf{v} is the particle's velocity and \mathbf{x} its position at time t . We assume that on the time scales of interest the particle practically does not move, i.e. it has a negligible displacement, so we can ignore the time dependence of \mathbf{x} . Thus, the particle's position \mathbf{x} is taken as constant in what follows [17].¹⁰ Assuming that the particle is initially at rest, integration of Eq. (3) gives

$$\mathbf{v}(\mathbf{x}, t) = \frac{q}{m} \int_{t_0}^t \mathbf{E}(\mathbf{x}, t') dt', \quad (4)$$

and the mean squared velocity, velocity dispersion or simply dispersion in each of the three independent directions $i = x, y, z$ is given by¹¹

$$\langle \Delta v_i^2 \rangle = \frac{q^2}{m^2} \int_{t_0}^t \int_{t_0}^t \langle E_i(\mathbf{x}, t') E_i(\mathbf{x}, t'') \rangle dt' dt''. \quad (5)$$

Following Yu and Ford [17], we assume that the electric field is a sum of classical \mathbf{E}_c and quantum \mathbf{E}_q parts. Because \mathbf{E}_c is not subject to quantum fluctuations and $\langle \mathbf{E}_q \rangle = 0$, the two-point function $\langle E_i(\mathbf{x}, t) E_i(\mathbf{x}', t') \rangle$ in equation (5) involves only the quantum part of the electric field [17].

It can be shown [61] that locally

$$\langle E_i(\mathbf{x}, t) E_i(\mathbf{x}', t') \rangle = \frac{\partial}{\partial x_i} \frac{\partial}{\partial x'_i} D(\mathbf{x}, t; \mathbf{x}', t') - \frac{\partial}{\partial t} \frac{\partial}{\partial t'} D(\mathbf{x}, t; \mathbf{x}', t') \quad (6)$$

¹⁰ The corrections arising from the inexactness of this assumption are negligible in the low velocity regime.

¹¹ By definition, $\langle \Delta v_i^2(\mathbf{x}, t) \rangle = \langle v_i^2(\mathbf{x}, t) \rangle - \langle v_i(\mathbf{x}, t) \rangle^2$.

where, in Minkowski spacetime, the Hadamard function $D(\mathbf{x}, t; \mathbf{x}', t')$ is given by

$$D_0(\mathbf{x}, t; \mathbf{x}', t') = \frac{1}{4\pi^2(\Delta t^2 - |\Delta \mathbf{x}|^2)}. \quad (7)$$

The subscript 0 indicates standard Minkowski spacetime $\mathbb{R} \times \mathbb{E}^3$, $\Delta t = t - t'$ and $|\Delta \mathbf{x}| \equiv r$ is the spatial separation for topologically trivial Minkowski spacetime:

$$r^2 = (x - x')^2 + (y - y')^2 + (z - z')^2. \quad (8)$$

B. The spacetime manifold

In this work, the time non-orientable spacetime manifold that we shall consider is of the form $\mathcal{M}_4 = \mathcal{M}^2 \times \mathbb{E}^2$ in which the first factor \mathcal{M}^2 is the non-orientable twisted cylinder \mathbb{C}^{*2} equipped with a Lorentz metric with time as the flipped coordinate. This makes \mathcal{M}^2 *time* non-orientable and, as a consequence, the spacetime manifold \mathcal{M}_4 is also time non-orientable. In Table II we show the time separation Δt and the spatial separation r that enter the spacetime interval $\Delta s^2 = \Delta t^2 - r^2$ in \mathcal{M}_4 for $\mathcal{M}^2 = \mathbb{C}^{*2}$ and $\mathcal{M}^2 = \mathbb{C}^2$, the cases treated in this paper. For $\mathcal{M}^2 = \mathbb{C}^{*2}$ the non-orientability is associated with the time coordinate.

Manifold	Time separation Δt	Spatial separation r^2
$\mathbb{C}^{*2} \times \mathbb{E}^2$	$t - (-1)^{n_x} t'$	$(x - x' - n_x a)^2 + (y - y')^2 + (z - z')^2$
$\mathbb{C}^2 \times \mathbb{E}^2$	$t - t'$	$(x - x' - n_x a)^2 + (y - y')^2 + (z - z')^2$

TABLE II. Time and space separation for the spacetime interval $\Delta s^2 = \Delta t^2 - r^2$ in the Hadamard function for the spacetime manifolds obtained by taking the Cartesian product with \mathbb{E}^2 of the two-dimensional manifolds \mathbb{C}^{*2} or \mathbb{C}^2 with coordinates t, x ; the coordinates associated with \mathbb{E}^2 are y, z . With time always in the first factor, each flat four-manifold thus obtained is endowed with a Lorentz metric with signature -2 . In the case of \mathbb{C}^{*2} the identification with inversion is made on the time direction, so that the corresponding spacetime is not time orientable. The topological compact spatial scale is denoted by a . The number n_x is an integer that runs from $-\infty$ to ∞ .

Let us try to make our terminology and notation as clear as possible. Being aware of the abuse of language but striving for simplicity, we henceforward give the name *twisted cylinder*, denoted by $\mathbb{C}^{*2} \times \mathbb{E}^2$, to the time non-orientable spacetime with coordinates (t, x, y, z) , whose points are identified as $(t, x, y, z) \equiv ((-1)^{n_x} t, x + n_x a, y, z)$, and equipped with the Lorentz metric $\Delta s^2 = \Delta t^2 - r^2$, where Δt and r are given in the first line of Table II. Similarly, we give the name *cylinder*, denoted by $\mathbb{C}^2 \times \mathbb{E}^2$, to the time orientable spacetime with coordinates

(t, x, y, z) , whose points are identified as $(t, x, y, z) \equiv (t, x + n_x a, y, z)$, and equipped with the Lorentz metric $\Delta s^2 = \Delta t^2 - r^2$, where Δt and r are given in the second line of Table II.

IV. TIME-ORIENTABILITY INDICATOR FOR THE TWISTED CYLINDER

We take up now the study of the stochastic motions of a charged particle under quantum vacuum electromagnetic fluctuations in the time non-orientable twisted cylinder $\mathbb{C}^{*2} \times \mathbb{E}^2$.

In a topologically nontrivial spacetime, the time interval Δt and the spatial separation r take new forms that capture the periodic boundary conditions imposed on the covering space. To obtain the correlation function for the electric field that is required to compute the velocity dispersion (5) for the twisted cylinder $\mathbb{C}^{*2} \times \mathbb{E}^2$, we replace in Eq. (6) the Hadamard function $D(\mathbf{x}, t; \mathbf{x}', t')$ by its renormalized version given by [20]

$$D_{ren}(\mathbf{x}, t; \mathbf{x}', t') = D(\mathbf{x}, t; \mathbf{x}', t') - D_0(\mathbf{x}, t; \mathbf{x}', t') = \sum_{n_x=-\infty}^{\infty \prime} \frac{1}{4\pi^2(\Delta t^2 - r^2)}, \quad (9)$$

where here and in what follows $\sum \prime$ indicates that the Minkowski contribution term $n_x = 0$ is excluded from the summation, and, according to Table II, the time and space separations for the time non-orientable spacetime $\mathbb{C}^{*2} \times \mathbb{E}^2$ are

$$\Delta t = t - (-1)^{n_x} t', \quad r^2 = (x - x' - n_x a)^2 + (y - y')^2 + (z - z')^2. \quad (10)$$

The term with $n_x = 0$ in the sum (9) is the Hadamard function $D_0(\mathbf{x}, t; \mathbf{x}', t')$ for standard Minkowski spacetime. This term has been subtracted out from the sum because it gives rise to an infinite contribution to the velocity dispersion.

Thus, from equation (6) the renormalized correlation functions

$$\langle E_i(\mathbf{x}, t) E_i(\mathbf{x}', t') \rangle_{ren} = \frac{\partial}{\partial x_i} \frac{\partial}{\partial x'_i} D_{ren}(\mathbf{x}, t; \mathbf{x}', t') - \frac{\partial}{\partial t} \frac{\partial}{\partial t'} D_{ren}(\mathbf{x}, t; \mathbf{x}', t') \quad (11)$$

are then given by

$$\langle E^i(\mathbf{x}, t) E^i(\mathbf{x}', t') \rangle_{ren}^{\mathbb{C}^{*2}} = \sum_{n_x=-\infty}^{\infty \prime} \frac{[3(-1)^{n_x} - 1]\Delta t^2 + [1 + (-1)^{n_x}]r^2 - 4r_i^2}{2\pi^2[\Delta t^2 - r^2]^3}, \quad (12)$$

where Δt and r^2 are given by Eq. (10), while

$$r_1 \equiv r_x = x - x' - n_x a, \quad r_2 \equiv r_y = y - y', \quad r_3 \equiv r_z = z - z'. \quad (13)$$

The orientability indicator $I_{v_i^2}^{\mathbb{C}^{*2}}$ that we will consider is defined by replacing the electric field correlation functions in Eq. (5) by their renormalized counterparts:¹²

$$I_{v_i^2}^{\mathbb{C}^{*2}}(\mathbf{x}, t, t_0) = \frac{q^2}{m^2} \int_{t_0}^t \int_{t_0}^t \left\langle E^i(\mathbf{x}, t') E^i(\mathbf{x}, t'') \right\rangle_{ren}^{\mathbb{C}^{*2}} dt' dt'' . \quad (14)$$

From (9) it is clear that the orientability indicator $I_{v_i^2}^{\mathbb{C}^{*2}}$ is the difference between the velocity dispersion in $\mathbb{C}^{*2} \times \mathbb{E}^2$ and the one in Minkowski spacetime with trivial topology.

Before moving on to explicit computations, a few words of clarification on the meaning of the indicator (14) are fitting. From equations (5) and (9) a general definition of the orientability indicator can be written in the form

$$I_{v_i^2}^{MC} = \left\langle \Delta v_i^2 \right\rangle^{MC} - \left\langle \Delta v_i^2 \right\rangle^{SC} , \quad (15)$$

where $\left\langle \Delta v_i^2 \right\rangle$ is the mean square velocity dispersion, and the superscripts *MC* and *SC* stand for multiply- and simply-connected manifolds, respectively. The right-hand side of (15) is defined by first taking the difference of the two terms with $\mathbf{x}' \neq \mathbf{x}$ and then setting $\mathbf{x}' = \mathbf{x}$.

On the face of it, the indicator (15) does not appear to be measurable because it involves the difference of quantities associated with two different spacetimes, but the spacetime we live in is unique. However, $I_{v_i^2}^{MC}$ is accessible by measurements performed in our spacetime, which is to be tested for time non-orientability, by the following procedure. First one would measure the velocity correlation function $\left\langle \Delta v_i(\mathbf{x}, t) \Delta v_i(\mathbf{x}', t) \right\rangle^{MC}$ for $\mathbf{x} \neq \mathbf{x}'$, then one would subtract out the correlation function $\left\langle \Delta v_i(\mathbf{x}, t) \Delta v_i(\mathbf{x}', t) \right\rangle^{SC}$ that has been *theoretically computed* for $\mathbf{x} \neq \mathbf{x}'$ for the corresponding topologically trivial Minkowski spacetime in the Appendix of Ref. [27]. Finally, the corresponding curve for the difference (15) as a function of time would be plotted in the coincidence limit $\mathbf{x} = \mathbf{x}'$.¹³

¹² To avoid a cluttered notation, for the superscript on the statistical indicator and on the electric field correlation functions we write just \mathbb{C}^{*2} instead of $\mathbb{C}^{*2} \times \mathbb{E}^2$.

¹³ This approach is analogous to one used in the search for spatial topology of the universe from discrete cosmic sources, called cosmic crystallography [62], in which a topological signature of 3-space is given by a constant times the difference $\Phi_{exp}^{MC}(s_i) - \Phi_{exp}^{SC}(s_i)$ of the expected pair separation histogram (EPSH), and the EPSH for the underlying simply connected covering manifold [63, 64], which can be theoretically computed in analytical form [63, 65].

A. Indicators for the twisted cylinder

The orientability indicator $I_{v_i^2}^{\mathbb{C}^{*2}}$ can be computed with the help of the integrals [20]

$$\begin{aligned} I_- &= \int_{t_0}^t \int_{t_0}^t dt' dt'' \frac{1}{[(t' - t'')^2 - r^2]^3} \\ &= \frac{3(t - t_0)}{16r^5} \ln \left[\left(\frac{t_0 - t + r}{t_0 - t - r} \right)^2 \right] + \frac{1}{4r^2 [(t - t_0)^2 - r^2]} + \frac{1}{4r^4} \end{aligned} \quad (16)$$

and

$$\begin{aligned} J_- &= \int_{t_0}^t \int_{t_0}^t dt' dt'' \frac{(t' - t'')^2}{[(t' - t'')^2 - r^2]^3} \\ &= \frac{(t - t_0)}{16r^3} \ln \left[\left(\frac{t_0 - t - r}{t_0 - t + r} \right)^2 \right] + \frac{1}{4[(t - t_0)^2 - r^2]} + \frac{1}{4r^2} \end{aligned} \quad (17)$$

as well as

$$\begin{aligned} I_+ &= \int_{t_0}^t \int_{t_0}^t dt' dt'' \frac{1}{[(t' + t'')^2 - r^2]^3} = \frac{3t_0}{16r^5} \ln \left[\left(\frac{2t_0 - r}{2t_0 + r} \right)^2 \left(\frac{t_0 + t + r}{t_0 + t - r} \right)^2 \right] + \frac{1}{8r^2 [4t_0^2 - r^2]} \\ &\quad + \frac{3t}{16r^5} \ln \left[\left(\frac{t_0 + t + r}{t_0 + t - r} \right)^2 \left(\frac{2t - r}{2t + r} \right)^2 \right] + \frac{1}{8r^2 [4t^2 - r^2]} - \frac{1}{4r^2 [(t + t_0)^2 - r^2]} \end{aligned} \quad (18)$$

and

$$\begin{aligned} J_+ &= \int_{t_0}^t \int_{t_0}^t dt' dt'' \frac{(t' + t'')^2}{[(t' + t'')^2 - r^2]^3} = \frac{t_0}{16r^3} \ln \left[\left(\frac{2t_0 + r}{2t_0 - r} \right)^2 \left(\frac{t_0 + t - r}{t_0 + t + r} \right)^2 \right] + \frac{1}{8[4t_0^2 - r^2]} \\ &\quad + \frac{t}{16r^3} \ln \left[\left(\frac{t_0 + t - r}{t_0 + t + r} \right)^2 \left(\frac{2t + r}{2t - r} \right)^2 \right] + \frac{1}{8[4t^2 - r^2]} - \frac{1}{4[(t + t_0)^2 - r^2]} \end{aligned} \quad (19)$$

By using these integrals and equations (12) and (13) in Eq. (14) we find

$$I_{v_i^2}^{\mathbb{C}^{*2}}(\mathbf{x}, t, t_0) = \frac{q^2}{\pi^2 m^2} \left\{ \sum'_{\text{even } n_x} [J_- + (r^2 - 2r_i^2)I_-] - 2 \sum_{\text{odd } n_x} [J_+ + r_i^2 I_+] \right\}. \quad (20)$$

where, since the coincidence limit $\mathbf{x} = \mathbf{x}'$ has been taken,

$$r_1 = -n_x a, \quad r_2 = r_3 = 0, \quad r^2 = r_1^2 + r_2^2 + r_3^2 = n_x^2 a^2, \quad (21)$$

as follows from Eq. (13) in the coincidence limit.

B. Indicators for the cylinder

We are looking for a local way to probe a putative time non-orientability of spacetime. To this end, let us compare the above results for the twisted cylinder $\mathbb{C}^{*2} \times \mathbb{E}^2$ manifold with those for its time-orientable counterpart, the cylinder $\mathbb{C}^2 \times \mathbb{E}^2 = \mathbb{R} \times \mathbb{S}^1 \times \mathbb{E}^2$. The indicators for the cylinder are given in Ref. [27] as¹⁴

$$I_{v_x^2}^{\mathbb{C}^2}(\mathbf{x}, t, t_0) = -\frac{q^2(t-t_0)}{4\pi m^2} \sum'_{n_x} \frac{1}{r^3} \ln \frac{(r-t+t_0)^2}{(r+t-t_0)^2}, \quad (22)$$

$$I_{v_y^2}^{\mathbb{C}^2}(\mathbf{x}, t, t_0) = I_{v_z^2}^{\mathbb{C}^2}(\mathbf{x}, t) = \frac{q^2(t-t_0)}{8\pi m^2} \sum'_{n_x} \left[\frac{4(t-t_0)}{r^2[(t-t_0)^2 - r^2]} + \frac{1}{r^3} \ln \frac{(r-t+t_0)^2}{(r+t-t_0)^2} \right], \quad (23)$$

where $r = n_x a$.

C. Locally probing time non-orientability

A significant difference between the case of the time non-orientable twisted cylinder and that of time-orientable spacetimes is that the indicator (20) depends both on t and t_0 , and not only on the difference $t - t_0$. This is because the twisted cylinder $\mathbb{C}^{*2} \times \mathbb{E}^2$ is not globally temporally homogeneous.

By means of a picture, we highlight the main consequences of the twisted cylinder's lack of global time homogeneity on the statistical indicator (20). In Fig. 1 we show two components of indicator (20) as functions of t, t_0 , with the indicator values represented by colors (the z -component of the indicator is not shown because it coincides with its y -component). Contour lines of the indicator are also displayed. Figs. 1 (a) and (b) illustrate the global temporal inhomogeneity of the twisted cylinder $\mathbb{C}^{*2} \times \mathbb{E}^2$: the patterns encountered as one moves horizontally along the t -axis are different for each fixed t_0 . The nontrivial contour curves are also quite different from those for $\mathbb{C}^2 \times \mathbb{E}^2$, which are the straight lines $t - t_0 = \text{const}$. There are periodic repetition patterns but with changing absolute value of the indicators. The topological singularity structure, indicated by the white straight lines, is also much richer than the one for the time orientable case. For example, the vertical lines $t = 1/2, 3/2, 5/2, \dots$ are singularities of topological nature that are not present in the indicators for the time orientable spacetime $\mathbb{C}^2 \times \mathbb{E}^2$.

¹⁴ In equations (26) and (27) of Ref. [27] the choice $t_0 = 0$ was made. Also, what we call here the cylinder is denoted there by E_{16} .

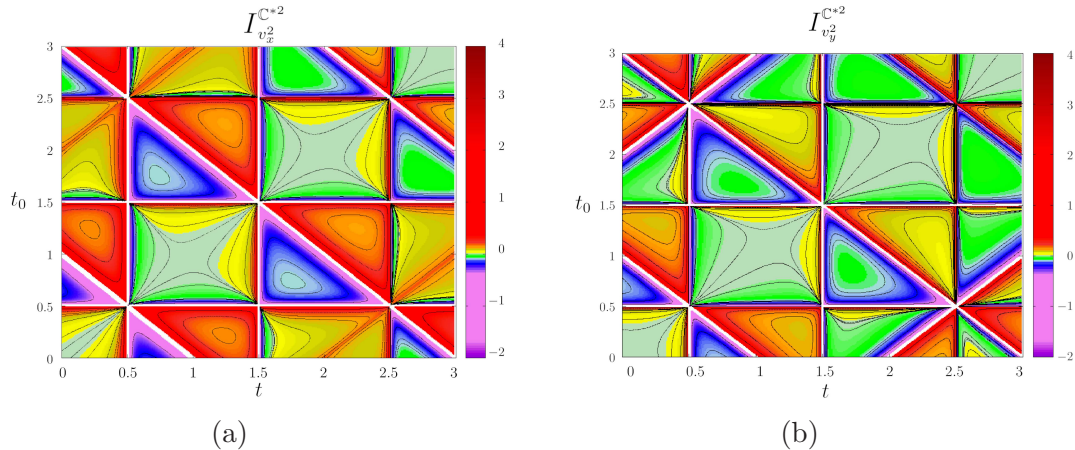


FIG. 1. Two components of indicator (20) as functions of t, t_0 . The values of the indicator are represented by colors. Panel (a) shows the x -component of the indicator (20), while panel (b) shows its y -component (the z -component is not displayed because it equals the y -component). Contour lines of the indicators are also exhibited. In these plots, q, m and a are all set to unity for qualitative reasons only. The white thin lines are topological singularities that arise for special values of t, t_0 , such as $t - t_0 = r, t + t_0 = r, t = r/2, t_0 = r/2$, where $r = |n_x|a$. The structure of singularities of topological origin is much richer than the one in the case of time-orientable spacetimes [20, 27, 28].

Figure 1 illustrates quite vividly how the global inhomogeneity of the twisted cylinder manifests itself through the statistical indicator (20). Next we study how the indicator (20) for the twisted cylinder behaves as a function of t for fixed t_0 . Figures 2 and 3 compare components of the indicator for $\mathbb{C}^{*2} \times \mathbb{E}^2$ with those for its time orientable counterpart $\mathbb{C}^2 \times \mathbb{E}^2$ for two values of t_0 . Both for $t_0 = 0$ (Fig. 2) and $t_0 = 1.3$ (Fig. 3) there appears an inversion pattern in the case of $\mathbb{C}^{*2} \times \mathbb{E}^2$, roughly of the form \cup followed by \cap . The absence of any inversion pattern in the case of the time-orientable $\mathbb{C}^2 \times \mathbb{E}^2$ allows one to pinpoint the temporally non-orientable case.

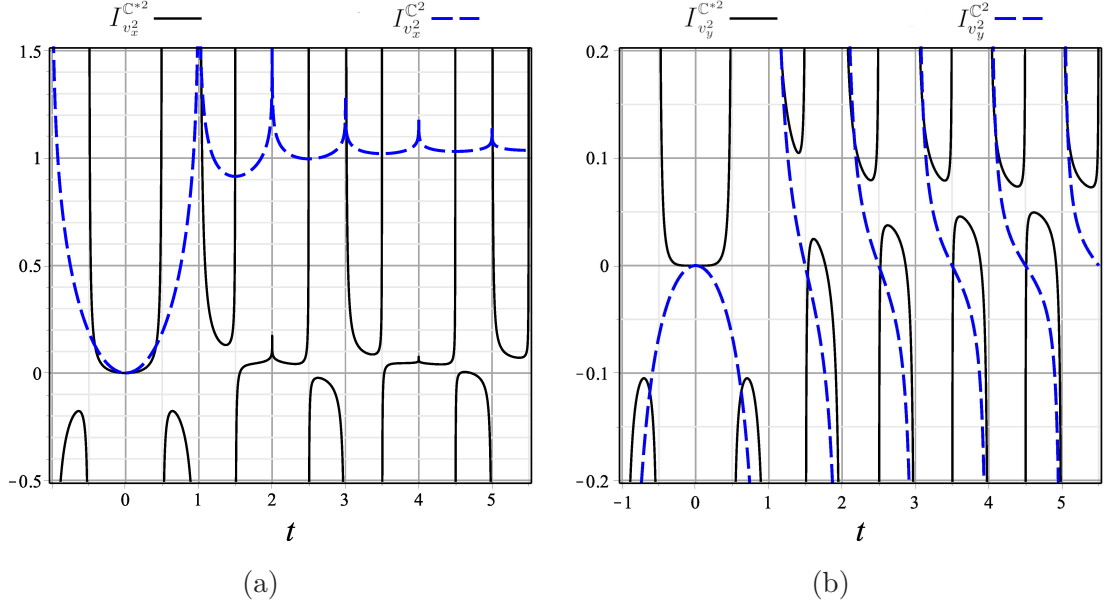


FIG. 2. Comparison of two components of the indicator for the twisted cylinder $\mathbb{C}^{*2} \times \mathbb{E}^2$ with those for its time orientable counterpart $\mathbb{C}^2 \times \mathbb{E}^2$. In both plots $t_0 = 0$. Panel (a) shows the x -component of the indicator for $\mathbb{C}^{*2} \times \mathbb{E}^2$ given by (20) plotted together with the x -component of the indicator for $\mathbb{C}^2 \times \mathbb{E}^2$ given by (23). Panel (b) shows the same comparison for the y -component of the indicator. In these plots, q , m and a are all set to unity for qualitative reasons only. The solid curves for $\mathbb{C}^{*2} \times \mathbb{E}^2$ present an inversion pattern, roughly of the form \cup followed by \cap , which is absent from the dashed curves for the time-orientable $\mathbb{C}^2 \times \mathbb{E}^2$.

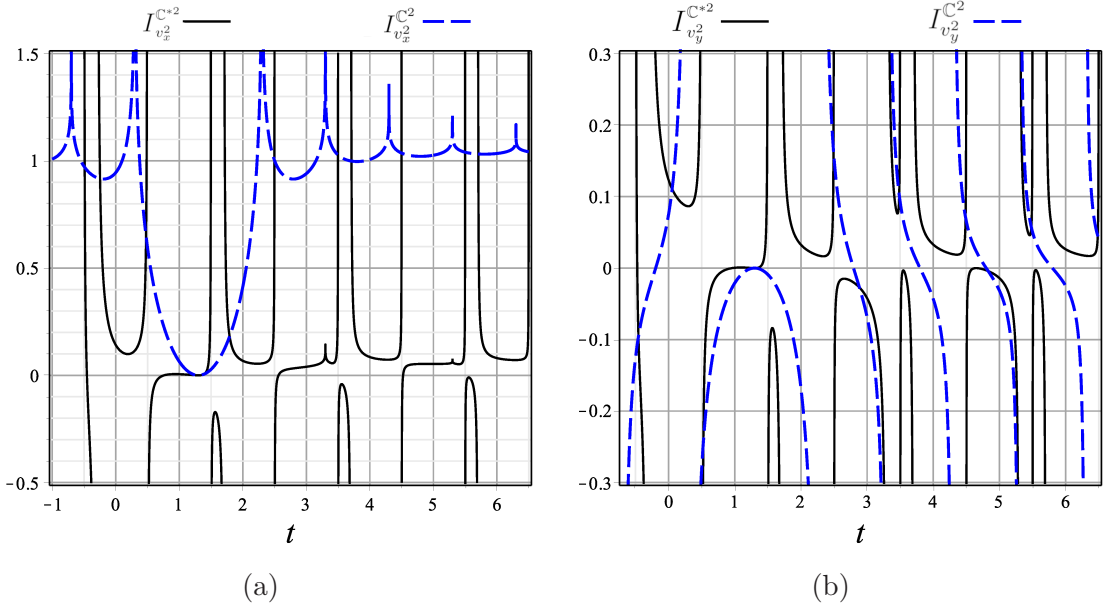


FIG. 3. The same as in Fig. 2 for $t_0 = 1.3$. Again, the solid curves for $\mathbb{C}^{*2} \times \mathbb{E}^2$ exhibit an inversion pattern, roughly of the form \cup followed by \cap , which is absent from dashed the curves for its time-orientable counterpart $\mathbb{C}^2 \times \mathbb{E}^2$.

V. SUMMARY OF RESULTS AND FINAL COMMENTS

In relativistic cosmology and quantum field theory, spacetime is assumed to be orientable as a topological manifold, and is additionally endowed with a Lorentz metric, making it separately time and space orientable. The question as to whether the laws of physics require that spacetime manifolds adhere to these orientability assumptions are among the unsettled issues in this framework. Although non-orientability is generally seen as an undesirable feature, non-orientable Lorentzian spacetime manifolds are concrete mathematical possibilities in physics at different scales. Therefore, the possibility that spacetime is time non-orientable ought not to be jettisoned forthwith. Strict orientability assumptions could potentially interfere with the understanding of fundamental aspects of the interplay of physics and topology. In fact, we do not know to what extent the topology of the underlying spacetime manifold might encode, or whether it is necessary to capture or express, basic features of the physical world in some scale. It is conceivable that topological properties such as global homogeneity and orientability of spacetime manifolds might be testable in both micro- and macro-physical scales. Previous speculations on time orientability violation have revolved about Gedanken experiments that would allegedly provide signatures a putative time non-orientability of spacetime [66, 67]. These ideas and other approaches to testing time orientability have been recently subjected to a searching critique [68]. Here, however, we have settled on probing the orientability of spacetime by means of measurable local physical effects.

Inasmuch as the role played by time orientability is more clearly accessed in static flat spacetime, whose dynamical degrees of freedom are frozen, in the present paper, instead of the expanding Friedmann–Lemaître–Robertson–Walker spacetime (FLRW), we have focused on the time orientability of Minkowski spacetime, leaving for a forthcoming article [69] some important related questions regarding the so-called arrow of time — observed time asymmetry in macrophysics and in the evolution of the universe, despite the time reversal invariance of the fundamental laws of physics. This includes, for example, whether temporal orientability of the FLRW universe can be probed and whether one can understand in a far-reaching context the several existing arrows of time [11, 15, 16].

In this paper we have argued that a presumed time non-orientability of Minkowski empty spacetime can be locally probed through physical effects associated with quantum vacuum electromagnetic fluctuations. To this end, we have studied the stochastic motions of a

charged particle under these fluctuations in Minkowski spacetime manifold, \mathcal{M}_4 , endowed with a time non-orientable topology (the twisted cylinder¹⁵ $\mathcal{M}_4 = \mathbb{C}^{*2} \times \mathbb{E}^2$) and its time orientable counterpart (the cylinder $\mathcal{M}_4 = \mathbb{C}^2 \times \mathbb{E}^2$) — see Tables I and II. We have found that the statistical topological indicator given by Eq. (14) is suitable to bring out the time non-orientability in the twisted cylinder case. Accordingly, we have derived analytical expressions for the statistical orientability indicator corresponding to Minkowski spacetime manifold \mathcal{M}_4 equipped with time non-orientable and its time orientable counterpart.

The chief conclusion of this work is reached through comparisons between the stochastic motions of a charged test particle in Minkowski spacetime endowed with each of the two spacetime topologies. Since the expressions for the orientability indicators — Eqs. (20), (22) and (23) — are too involved for a direct comparison, to demonstrate our main result, which is ultimately stated in terms of patterns of curves for the orientability indicators, we have performed numerical computations and plotted figures for the components of our statistical orientability indicator.

Figure 1 aims to illustrate the topological temporal inhomogeneity for \mathcal{M}_4 corresponding to the twisted cylinder $\mathbb{C}^{*2} \times \mathbb{E}^2$, a feature not shared by the cylinder $\mathbb{C}^2 \times \mathbb{E}^2$. The patterns encountered are different for each fixed t_0 , and the closed contour curves are also quite different from those for $\mathbb{C}^2 \times \mathbb{E}^2$, which are straight 45-degree lines. The topological singularity structure is also markedly richer than the one for the time orientable case.

However, the answer to the central question of the paper, namely how to locally probe the time orientability of Minkowski intrinsically, is accomplished by comparing the time evolution of the orientability indicators $I_{v_i^2}^{\mathbb{C}^{*2}}$ and $I_{v_i^2}^{\mathbb{C}^2}$. Indeed, Figs. 2 and 3 show that it is possible to locally unveil time non-orientability through the inversion pattern of curves of the time non-orientability indicator for a charged particle under quantum vacuum electromagnetic fluctuations. This inversion pattern is a signature of time non-orientability and is absent in the time orientable case.

It should be noticed that the time non-orientability considered in this paper is of topological origin. It is different from the existence of closed timelike curves in Gödel and other spacetime solutions of Einstein's equations [70]. In the Gödel model, for example, gravity tilts the local light cones over extended spacetime regions so as to allow continuous closed

¹⁵ We recall that a visualization of the twisted cylinder is provided by the Möbius band, a representation that is somewhat inaccurate but can be realized in three-dimensional space.

timelike curves — there is no periodic time inversion of topological origin.

To summarize, the main result of our analysis is that it may be feasible to look into a conceivable topological time non-orientability of Minkowski empty spacetime by measurable local physical effects associated with quantum vacuum electromagnetic fluctuations.

ACKNOWLEDGMENTS

M.J. Rebouças acknowledges the support of FAPERJ under a CNE E-26/202.864/2017 grant, and thanks CNPq for the grant under which this work was carried out. We are grateful to A.F.F. Teixeira for a careful reading of the manuscript and discussions.

-
- [1] S.W. Hawking and G.F.R. Ellis, *The Large Scale Structure of Space-Time* (Cambridge University Press, Cambridge, 1973).
 - [2] R. Geroch and G.T. Horowitz, *Global structure of spacetimes in General relativity: An Einstein centenary survey*, pp. 212-293, Eds. S. Hawking and W. Israel (Cambridge University Press, Cambridge, 1979).
 - [3] E. Minguzzi, *Lorentzian causality theory*, Living Rev Relativ **22**, 3 (2019).
 - [4] J.R. Weeks, *The Shape of Space*, 3rd ed. (CRC Press, Boca Raton, FL, 2020).
 - [5] Wikipedia: Orientability, available at: <https://en.wikipedia.org/wiki/Orientability> (Accessed: 21 August 2022).
 - [6] Ya. B. Zeldovich and I.D. Novikov, JETP Letters **6**, 236 (1967).
 - [7] R. Penrose, The Structure of Space-Time, in *Battelle Rencontres in Mathematics and Physics: Seattle, 1967*, C. M. DeWitt and J. A. Wheeler, Eds. (Benjamin, New York, 1968).
 - [8] R. Penrose and W. Rindler, *Spinors and Space-time, Volume 1, Two-spinor calculus and relativistic fields* (Cambridge University Press, Cambridge, 1986).
 - [9] R. Geroch, J. Math. Phys. **9**, 1739 (1968).
 - [10] R. Geroch, J. Math. Phys. **9**, 343 (1970).
 - [11] G.F.R. Ellis and B. Drossel, Found. Phys. **50**, 161 (2020).
 - [12] M. Castagnino, L. Lara and O. Lombardi, Class. Quantum Grav. **20**, 369 (2003).
 - [13] H. Reichenbach *The Direction of Time*, University of California Press, Berkeley 1971.
 - [14] P.C.W. Davies, *The Physics of Time Asymmetry*, University of California Press, Berkeley-Los Angeles, 1974.
 - [15] J. Barbour, *The End of Time: The Next Revolution in Physics*, Oxford University Press, Oxford (2001).
 - [16] C. Rovelli, *The Order of Time*, Riverhead Books, USA 2018.
 - [17] H. Yu and L.H. Ford, Phys. Rev. D **70**, 065009 (2004). doi:10.1103/PhysRevD.70.065009. URL <http://dx.doi.org/10.1103/PhysRevD.70.065009>
 - [18] G. Gour and L. Sriramkumar, Found. Phys. **29**, 1917 (1999).
 - [19] M.T. Jaekel and S. Reynaud, Quant. Opt. **4**, 39 (1992).
 - [20] C.H.G. Bessa and M.J. Rebouças, Class. Quant. Grav. **37**(12), 125006 (2020). doi: 10.1088/1361-6382/ab848a. URL <http://dx.doi.org/10.1088/1361-6382/ab848a>

- [21] H.w. Yu and J. Chen, Phys. Rev. D **70**, 125006 (2004). doi:10.1103/PhysRevD.70.125006. URL <https://journals.aps.org/prd/abstract/10.1103/PhysRevD.70.125006>
- [22] L.H. Ford, Int. J. Theor. Phys. **44**, 1753 (2005). doi:10.1007/s10773-005-8893-z. URL <http://dx.doi.org/10.1007/s10773-005-8893-z>
- [23] H.w. Yu and J. Chen, P.x. Wu, JHEP **02**, 058 (2006). doi:10.1088/1126-6708/2006/02/058. URL <http://dx.doi.org/10.1088/1126-6708/2006/02/058>
- [24] M. Seriu and C.H. Wu, Physical Review A **77**(2) (2008). doi:10.1103/physreva.77.022107. URL <http://dx.doi.org/10.1103/PhysRevA.77.022107>
- [25] V. Parkinson and L.H. Ford, Phys. Rev. A **84**, 062102 (2011). doi:10.1103/PhysRevA.84.062102. URL <http://dx.doi.org/10.1103/PhysRevA.84.062102>
- [26] V.A. De Lorenci, C.C.H. Ribeiro and M.M. Silva, Phys. Rev. D **94**(10), 105017 (2016). doi:10.1103/PhysRevD.94.105017. URL <http://dx.doi.org/10.1103/PhysRevD.94.105017>
- [27] N.A. Lemos, M.J. Rebouças, Eur. Phys. J. C **81**(7), 618 (2021). doi:10.1140/epjc/s10052-021-09426-9. URL <http://dx.doi.org/10.1140/epjc/s10052-021-09426-9>
- [28] N.A. Lemos, D. Müller and M.J. Rebouças, Phys. Rev. D **106**, 023528 (2022)
- [29] J.A. Wolf, *Spaces of Constant Curvature* (McGraw-Hill, New York, 1967).
- [30] W.P. Thurston, *Three-Dimensional Geometry and Topology. Vol.1*, Edited by Silvio Levy (Princeton University Press, Princeton, 1997).
- [31] C. Adams and J. Shapiro, American Scientist **89**, 443 (2001).
- [32] B. Cipra, *What's Happening in the Mathematical Sciences* (American Mathematical Society, Providence, RI, 2002).
- [33] A. Riazuelo, J. Weeks, J.P. Uzan, R. Lehoucq and J.P. Luminet, Phys. Rev. D **69**, 103518 (2004).
- [34] H. Fujii and Y. Yoshii, Astron. Astrophys. **529**, A121 (2011).
- [35] G.F.R. Ellis, Gen. Rel. Grav. **2**, 7 (1971). doi:10.1007/BF02450512. URL <http://dx.doi.org/10.1007/BF02450512>
- [36] M. Lachièze-Rey and J.P. Luminet, Phys. Rep. **254**(3), 135 (1995). doi:https://doi.org/10.1016/0370-1573(94)00085-H. URL <https://www.sciencedirect.com/science/article/pii/037015739400085H>
- [37] G.D. Starkman, Class. Quant. Grav. **15**, 2529 (1998). doi:10.1088/0264-9381/15/9/002. URL <http://dx.doi.org/10.1088/0264-9381/15/9/002>
- [38] J. Levin, Phys. Rep. **365**(4), 251 (2002). doi:10.1016/S0370-1573(02)00018-2. URL <https://www.sciencedirect.com/science/article/pii/S0370157302000182>
- [39] M.J. Rebouças and G.I. Gomero, Braz. J. Phys. **34**, 1358 (2004). doi:10.1590/S0103-97332004000700012. URL <https://www.scielo.br/j/bjp/a/DPsmZZVfnnqxb4q8NTPf8q/?lang=en&format=html>
- [40] M.J. Rebouças, A Brief Introduction to Cosmic Topology, in *Proc. XIth Brazilian School of Cosmology and Gravitation*, eds. M. Novello and S.E. Perez Bergliaffa (Americal Institute of Physics, Melville, NY, 2005).
- [41] J.P. Luminet, Universe **2**(1), 1 (2016). doi:10.3390/universe2010001. URL <http://dx.doi.org/10.3390/universe2010001>
- [42] P.A.R. Ade, N. Aghanim, C. Armitage-Caplan, M. Arnaud, M. Ashdown, F. Atrio-Barandela, J. Aumont, C. Baccigalupi, A.J. Banday, et al., Astronom. Astrophys. **571**, A16 (2014). doi:10.1051/0004-6361/201321591. URL <http://dx.doi.org/10.1051/0004-6361/201321591>
- [43] P.A.R. Ade, N. Aghanim, M. Arnaud, M. Ashdown, J. Aumont, C. Baccigalupi, A.J. Banday, R.B. Barreiro, J.G. Bartlett, et al., Astronom. Astrophys. **594**, A13 (2016). doi:10.1051/0004-6361/201525830. URL <http://dx.doi.org/10.1051/0004-6361/201525830>
- [44] N.J. Cornish, D.N. Spergel, G.D. Starkman and E. Komatsu, Phys.

- Rev. Lett. **92**, 201302 (2004). doi:10.1103/PhysRevLett.92.201302. URL <https://journals.aps.org/prl/abstract/10.1103/PhysRevLett.92.201302>
- [45] J. Shapiro Key, N.J. Cornish, D.N. Spergel and G.D. Starkman, Phys. Rev. D **75**, 084034 (2007). doi:10.1103/PhysRevD.75.084034. URL <https://journals.aps.org/prd/abstract/10.1103/PhysRevD.75.084034>
- [46] P. Bielewicz and A.J. Banday, Mon. Not. Roy. Astron. Soc. **412**, 2104 (2011). doi:10.1111/j.1365-2966.2010.18057.x. URL <https://academic.oup.com/mnras/article/412/3/2104/1058423>
- [47] P.M. Vaudrevange, G.D. Starkman, N.J. Cornish and D.N. Spergel, Phys. Rev. D **86**, 083526 (2012). doi:10.1103/PhysRevD.86.083526. URL <http://dx.doi.org/10.1103/PhysRevD.86.083526>
- [48] R. Aurich and S. Lustig, Mon. Not. Roy. Astron. Soc. **433**, 2517 (2013). doi:10.1093/mnras/stt924. URL <https://academic.oup.com/mnras/article/433/3/2517/1235728>
- [49] G.I. Gomero, B. Mota and M.J. Rebouças, Phys. Rev. D **94**(4), 043501 (2016). doi: 10.1103/PhysRevD.94.043501. URL <http://dx.doi.org/10.1103/PhysRevD.94.043501> .
- [50] M.A. Henle, *Combinatorial Introduction to Topology*, pp. 100–111. Dover, New York (1994).
- [51] J. Stillwell, *Geometry of Surfaces*, Springer-Verlag New York, Inc. (1992).
- [52] B.S. DeWitt, C.F. Hart and C.J. Isham, Physica **96A**, 197 (1979).
- [53] J.S. Dowker and R. Critchley, J. Phys. A **9**, 535 (1976).
- [54] P.M. Sutter and T. Tanaka, Phys. Rev. D **74**, 024023 (2006).
- [55] M.P. Lima and D. Müller, Class. Quant. Grav. **24**, 897 (2007).
- [56] D. Müller, H.V. Fagundes and R. Opher, Phys. Rev. D **66**, 083507 (2002).
- [57] D. Müller, H.V. Fagundes and R. Opher, Phys. Rev. D **63**, 123508 (2001).
- [58] D. Martin, *Manifold Theory: Introduction for Mathematical Physicists* (Horwood Publishing, West Sussex, 2002).
- [59] B. O’Neill, *Semi-Riemannian Geometry with application to Relativity*, Academic Press (1983).
- [60] F.J. Palomo and A. Romero, *Certain actual topics on modern Lorentzian geometry in Handbook of differential geometry*, vol II, p.pp 516-546 (2006). Eds. F.J.E. Dillen and L.C. A Verstraelen.
- [61] N.D. Birrel and P.C.W. Davies, *Quantum Fields in Curved Space* (Cambridge University Press, Cambridge, 1982).
- [62] R. Lehoucq, M. Lachièze-Rey and J.-P. Luminet, *Astron. Astrophys.* **313**, 339 (1996).
- [63] G.I. Gomero, M.J. Rebouças and A.F.F. Teixeira, Class. Quantum Grav. **18**, 1885 (2001).
- [64] G.I. Gomero, A.F.F. Teixeira, M.J. Rebouças and A. Bernui, Int. J. Mod. Phys. D **11**, 869 (2002).
- [65] M.J. Rebouças Int. J. Mod. Phys. D **9** 561 (2000).
- [66] M. Hadley, Class. Quantum Grav. **19**, 4565 (2002).
- [67] M. Hadley, *Testing the Orientability of Time*. Preprints 2018040240 (2018).
- [68] M. Bielińska and J. Read, *Testing Spacetime Orientability*, Foundations of Physics (2022) (forthcoming).
- [69] N.A. Lemos, D. Müller and M.J. Rebouças, *Probing time orientability of Friedmann-Robertson-Walker spacetime* (in preparation).
- [70] K. Gödel, Rev. Mod. Phys. **21**, 447 (1949).